

A New Pediatric Bone Age Assessment Using Cluster based Lightweight U-Net Architecture Multi-Scale Convolutional Network

Rakesh Kumar, Aasheesh Shukla

*Department of Computer Engineering & Applications
Department of Electronics & Communication Engineering
GLA, University, Mathura, India-281406
rakesh.kumar@gla.ac.in ,diwakar.bhardwaj@gla.ac.in*

Article Info

Volume 82

Page Number: 73 - 84

Publication Issue:

January-February 2020

Abstract

For diagnosis, major indicator is age of bone and it is used to find timing of various diseases. Growth and development are computed using bone age assessment, in addition to that used to diagnose and treat childhood diseases mainly with the use of X-ray images. Also it considered as the contemporary standard clinical practice for diagnosing metabolic and endocrine disorders in childhood development. The outcome says that every single age can be estimated by looking at the bones of the child if the infant has this skeleton and what old the baby is. The main reason for this BAA is to know how the bone grows when the child develops. Segmentation of the hand bone is mainly needed at this point to explain the properties of the hand bone in detail in medical records with x-ray images. The newly developed lightweight multi-scale U-Net convolutional neural network is used with x-ray images in a previous study for the betterment analysis of BAA. Today, however, this approach is limited to segmentation maps in pixel forms and it has been addressed by developing a new model based on profound education that considers the field of interest within and outside the field and the dimensions of the borders during the training using K-mean clustering algorithms as a pre-segmentation constraint. U-Net architecture forms the base for design of lightweight hand bone of children and better results of segmentation is achieved by this, especially for BAA segmentation of hand's small bones. For both learning and analysis this method requires images of the entire hands and various parts of the body. This method allows to measure the significance of the automatic examination of the age of the bone of each hand of x-ray images. The proposed approach allows for measurement of age of bone using other common methods while further evaluating the quality of the proposed method during developmental stages.

Keywords: *k-means, X-ray, segmentation of hand bones, multi-scale convolutional network, U-Net, bone age assessment.*

Article History

Article Received: 14 March 2019

Revised: 27 May 2019

Accepted: 16 October 2019

Publication: 01 January 2020

1 Introduction

The Bone Age Assessment (BAA) could be a pediatric radiological examination to see any mismatch between a child's age as per date of birth and skeletal age which is bones age. Pediatricians these days have depended for > seventy five years on techniques to see skeletal maturation.

Pediatricians got to be acutely aware that skeletal maturity assessments currently have broader applications, starting from alternative of elite sports and forensics to programs for world immigration. For example, several asylum seekers are required to expertise an age survey which will govern placement and resource access.

Bone age remains a helpful instrument for evaluating the health of kids. New technology for authoritative age involves computer-automated measurements and evaluations from different modalities of imaging. What is more, new applications for non-clinical bone age are developing, significantly regarding immigration and asylum rights for kids. Many of the fashionable techniques of authoritative bone age may be graduated to individual populations and promise higher performance across a wider spectrum of ethnicities, though a lot of info is needed.

Bone age is a sign of a personality's skeletal and biological development. This can be distinct from the written record era calculated victimization a personality's date of birth. Pediatricians and endocrinologists typically raise age to be compared with chronological age for the designation of sicknesses that end in youngsters of high or short stature. Serial measurements are accustomed appraise the effectuality of those diseases interventions.

If proper records of birth are not provided, age is estimated using computation of age of bone. Absent

birth information could be a massive downside in a part of the globe. In South Asia, 65th of all births aren't registered by age of five years. Therefore want for correct estimation mature arises in conditions wherever the age of a baby must be correct, like in competitive sports, in law suits and throughout immigration [4]. In this conditions bone age is employed to supply the nearest estimate of chronological age.

In BAA, the emergence of little hand bones, significantly small ossification centers in carpal bones and hollow bone epiphysis, are essential for assessing age, significantly for kids 0-7 years mature. Here steered a light-weight U-Net multi-scale convolutional network for precise segmentation outcomes of hand bones in X-ray. Numerous numbers of down sampling activities taken in U-Net design are calculable for the assignment of hand bones segmentation and during this study is go together with two. to boot, as hand bones grow larger in children's development (Figure 3.1), the mixture of kernels of identical size won't forever counteract variations within the bone scale.

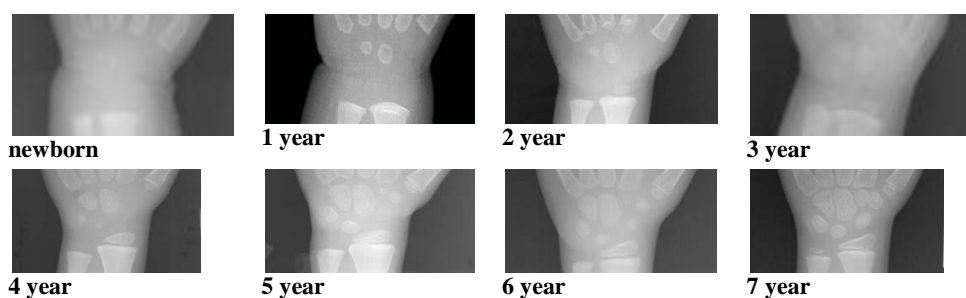


Figure 3.1. Carpal bones growth pattern from newborn to 7-year-old

Various methods were created that used distinct skeletal components as well as distinct visualization techniques to calculate bone age. Age of Bone is determined through matching subject's left wrist X-rays with the closest matching relation x-rays given in atlas that are normal for distinct ages given in atlas [1]. According to radiographs, this method is quick as well as easy. Standards of GP atlas in Australia as well as the Middle East are deemed

applicable and reliable to kids. Furthermore, there is a difference between both computed age of bone as well as age of chronological while applying this technique to Asian children [2].

By comparison, Tanner & Whitehouse (TW) technique is not affected by era, but on the maturity level of 20 chosen areas of concern (ROI) in particular neck or hand bones in each age group. Every other ROI's level of growth is classified into

particular phases marked as (A, B, C, D,...,I). Almost every phase of growth is provided a numerical rating on each bone separately. A complete maturity score is calculated by summarizing all of these results from those in the ROIs. For men and women, that little score is associated independently with bone age. The TW technique is relatively more complicated and needs some time; furthermore, comparative to the GP technique it will be more precise and reproducible[3].

Ago saying, idealized version and artificial images were generated specifically for skeletal maturity age and sex standards through extensively examining density of ossification centers and its morphology, shape, size in healthy children's hand X-rays and producing images including typical developmental qualities for every centers of ossification [4]. Pictures of older GP atlas are not accurate than fresh GR atlas pictures and have a better performance. All such fresh GR requirements are also spaced at periodic 6 monthly intervals between 2 and 6 years and at annual intervals between 7 and 17 years.

It was noted that in evaluating bone age from the GP as well as GR atlas, both pediatric endocrinologists and radiologists reported almost identical outcomes. Furthermore, there was an enhanced amount of outliers in the GR atlas. Then it can be seen as a substitute for the older GP atlas. A start-up module for processing visual data at different scales was suggested in [5]. Determined by the above, a multi-scale block is implemented to extract scale-relevant characteristics with distinct kernel sizes. With that of the precision of tiny bones identification, we assess the capacity of distinct networks to segment tiny bones. This would be the deep learning study of first-hand bone segmentation and the findings suggest promising performance in the segmentation of hand bones, particularly for tiny hand bones. So, for extracting scale-relevant features, multi-scale

block with various size of kernel introduced by this work. Detection accuracy of small bones are used to evaluate the performance of various networks used to segment small bones. With deep learning, this is the first method of segmentation of hand bone. In segmentation of hand bone, better results are produced by this, specifically in hand's small bone segmentation.

2 Proposed Methodology

The work's primary contribution is to propose a lightweight multi-scale convolutional U-Net architecture network to finish the segmentation of hand bones with k-means clustering. The U-Net architecture forms base for this compact design with two up and down-sampling activities and the adoption of various filters with distinct kernel sizes to counteract differences in the hand bone scale during children's development. Here use K-means clustering for segmenting picture into primary and then use U-net architecture for smooth born segmentation. It will assist decrease process complexity and achieve high precision compared to current methods. They compare various numbers of U-Net architecture up and down-sampling activities to achieve greater efficiency in the segmentation of hand bones. In specific, to obtain the scale-relevant characteristics, that also consists of various filters with distinct kernel size, multi-scale block is adapted which will be like Inception approach. Then maybe the network segments the end-to-end hand bones. Figure 1 shows the suggested architecture diagram. For pediatric hand bone X-ray, this work provides a lightweight multi-scale U-Net convolutional network with k-means cluster-based segmentation. With deep learning, it is the first study of segmentation of hand bone segmentation in addition outcomes of the experimentation shows auspicious results in the segmentation of hand bones, particularly for tiny hand bones.

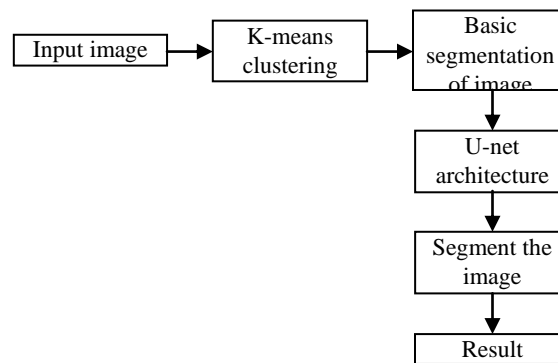


Figure 1. Proposed Architecture Diagram

3.1.1. Basic Segmentation of Bone image using k-means clustering

K-means Clustering Algorithm: K-means application is for segmenting picture into K clusters. This method includes few measures for dividing input picture data into the complete amount of clusters. It should be observed that distinct places result in distinct outcomes in K-means methods. Furthermore, points are obtained sequentially based on information to use K-means technique. Main age group is represented at end and fresh K [6] needs to be calculated. Data are classified according to their own information based on K-Means technique. This classification depends on the assessment of numerical data values. The algorithm will therefore automatically prepare an autonomous categorization without human oversight. The K-means algorithm could usually work with samples on an ongoing basis; furthermore, it can act as discrete data [7]. Collation between every line value is allowed by k-means to create clusters and classify samples where the line is based on range measurements. Pattern attribute dependency between each other is computed by using Euclidean distance in k-means technique. Based on characteristics provided by table, his distance is computed. Algorithm calculates

centroid on each of the clusters following the initial distance calculation. Even though the algorithm passes through each section, each centroid's value is recalculated based on the mean values of every pattern attribute in that centroid. While still, algorithm outcomes with k centroids. It places table patterns in line with its centroid distance [8]. The K-means method is shown as proceeds to demonstrate operation of algorithm:

Step 1: Begin with choice on significance of k, such as getting table's first k samples, devoting every resulting (N-k) sample to cluster.

Step 2: Between pattern and every centroid, distance matrix is created where heavy calculation is the challenge of this phase implies. Algorithm must assess $N \times K$ distances, if we k centroids and N samples.

Step 3: Place every sample in nearest centroid cluster and, if sample is not in the closest centroid cluster, move to that cluster.

Step 4: Reinstall fresh k centroids to every cluster that will be a centroid for the revised place.

Step 5: Reiterate until the condition of isotropy is met [9].

Above procedure is shown in Figure 3.3.

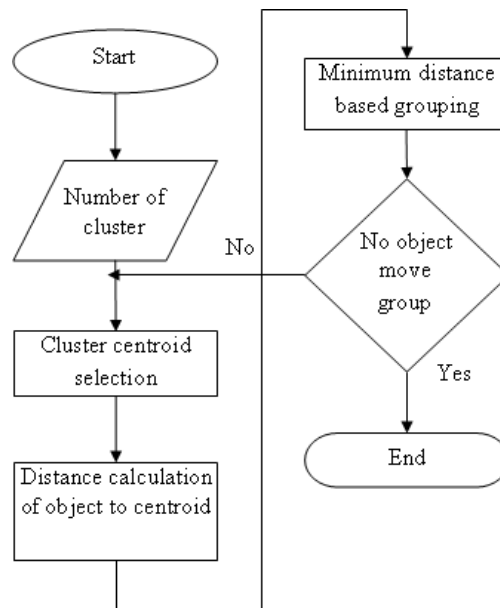


Figure 3.3: K-means process's block diagram

Using K-means unsupervised clustering method, two and three regions are formed by grouping the picture of X-ray. Regions represents region of soft tissue region with background, area of soft tissue with bone and bone with “K” equaling two or three. Objective function is optimized for performing this clustering integration. Squared error function is reduced by this and it is given by,

$$\sum_{j=1}^{\mathfrak{K}} \sum_{i=1}^n \|x_i^j - c_j\|^2 \quad (3.1)$$

Where, number of input data set is represented as n , clusters number is represented by \mathfrak{K} , $\|x_i^j - c_j\|^2$ is the distance quantity among the data point x_i^j which signifies image pixel's intensity value and Every group of pixel's mean value is computed to calculate cluster center c_j . Step by step algorithm of k-means cluster based bone segmentation is assumed as follows:

Input: X-ray image dataset (image pixels intensity) $\{x_i\}_1^n$, where, X-ray image of bone, total number of pixels is represented by n .

Initialization: The number of clusters 'k', $2 \leq \mathfrak{K} \leq 3$ where, integer is given by \mathfrak{K} , center of cluster, c_j , $1 < j \leq k$, iteration $T=0$, Set the tolerant error value ' ∂ ', $k=2$, $T=0$, $j=1$ and $i=1$

2: using Euclidean distance formula, value of cluster center and intensity are computed as:

$$\mathfrak{D}_{ij}^T = \sum_{j=1}^{\mathfrak{K}} \sum_{i=1}^n \|x_i^j - c_j^{T-1}\|^2$$

3: Dispense each data point here represented as intensity of pixel significance to center of cluster:

$$w_{ij} = \begin{cases} 1 & \text{argmin}_{j=1}^k \mathfrak{D}_{ij}^T \\ 0 & \text{else} \end{cases}$$

4: Finding new cluster center by recalculation of the cluster center:

$$c_j^T = \frac{\sum_i^n w_{ij}^T x_i}{\sum_i^n w_{ij}^T}$$

5: Ending standards testing: until tolerant error value ‘ ∂ ’ is greater than $\mathcal{E}(T)$, iteration process is repeated.

$$\mathcal{E}(T) = \|c_j^T - c_j^{T-1}\| \leq \partial$$

6: If ending condition is not reached, reiterate from step 2 with increased T value by 1.

7: With zero intensity, cluster blocks the pixels by assigning center of cluster as subordinate value. With center of cluster’s sophisticated value, intensity of pixels are maintained.

$$x_i^j = \begin{cases} 0 & \text{argmin}_{j=1}^2 C_j \\ x_i & \text{else} \end{cases}$$

8: Repeat the process with $k=3$

9: Block up the pixels be owned by clusters of lower value of cluster center with zero intensity and endure the pixels intensity for pixels that belongs to cluster.

$$x_i^j = \begin{cases} x_i & \text{argmin}_{j=1}^3 C_j \\ 0 & \text{else} \\ 0 & \text{else} \end{cases}$$

Output: K-means clustering with k value will be employed on each region for Figure 3.1 with cluster center’s high value and prior segmentation result is obtained.

3.1.2. Lightweight U-Net Architecture

For greater segmentation precision, the amount of up and down-sampling activities on pyramid shaped networks relies on particular issue. Hence, various amount of U-Net architecture with up and down-sampling activities is compared to discover a particular network with lightweight framework for segmentation of hand bone. Figure 3 illustrates initial U-Net (U-Net4) accepted for Input image size

of 256* 256. This has consecutive implementation of two 3x3 convolutions, every one is accompanied with linear rectified unit (ReLU)[12] and a 2x2 max downsampling procedure with stride 2. Feature map is up sampled in every phase of extensive path. It follows 2x2 convolution with number channels of feature. These channels are concatenated with from contracting path of respective feature map which is cropped. ReLU accompanies every path.

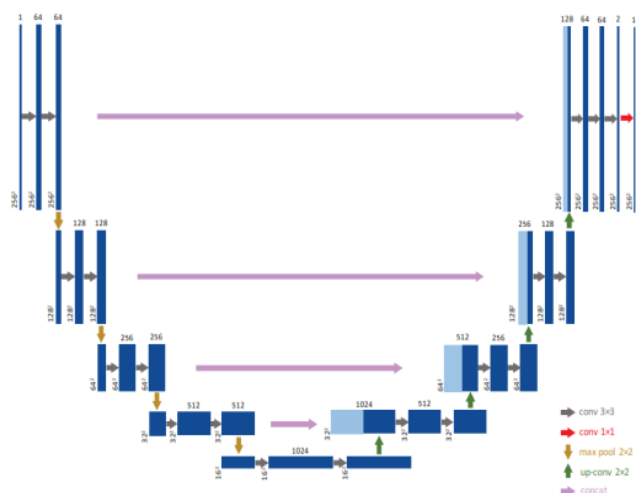


Figure 3.3. U-Net architecture with 4 up and down-sampling operations (U-Net⁴)

At final layer, 1x1 convolution is used to form required class number by mapping every 64-component feature vector. Various U-Net architectures contrasted with distinct downsampling

and upsampling activities (Figure 3.4) and U-Net[10] to segment same hand bone assignment and discovered that U-Net2 could achieve ideal efficiency.

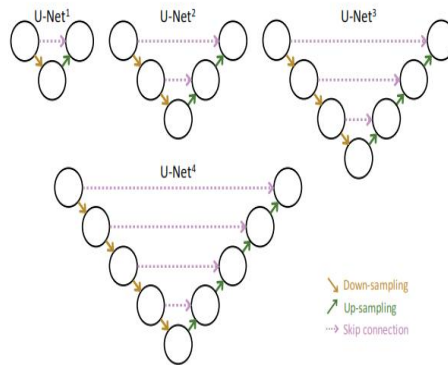


Figure 4. Various Number of up and down-sampling operations U-Net architectures

3.1.3. Multi-Scale Network Architecture

a multi-scale convolutional neural network (msCNN) have developed according to architecture of U-Net2 to compute hand bone's density maps from of distinct dimensions (Figure 5) [11]. A traditional 9-99 kernel-size convolution layer corresponds to first convolutional to restore the feature of image. Multi-Scale Blob (MSB) is used as an Inception-like model composed of various filters with distinct kernel sizes (including 3, 5, 7, 77 and 99).

ReLU is implemented as activation function of prior convolution layers except last one after each convolution layer [12]. Table 1 shows detailed

settings of parameters. Single kernel dimensions are substituted to MSB, in order to assessing efficiency of segmentation with MSB (3regional, 5regional, 7regional and 9regional). For 4 single size kernel networks, test the outcomes of segmentation individually. Dice coefficient loss function is used to compute energy function, which is done by sigmoid activation function over final map of feature. Dice coefficient is expressed as,

$$\frac{2 * S_1 * S_2}{S_1 + S_2} \quad (1)$$

where S_1 is result of segmentation result and S_2 is ground truth.

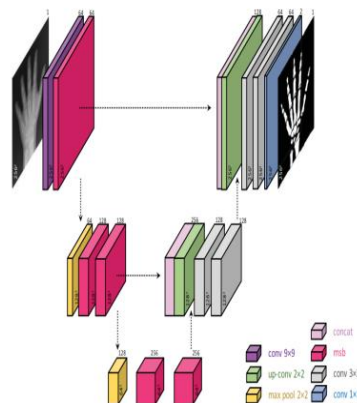


Figure 5. U-Net² based lightweight U-Net architecture multi-scale convolutional network for segmentation of pediatric hand bone in X-ray image.

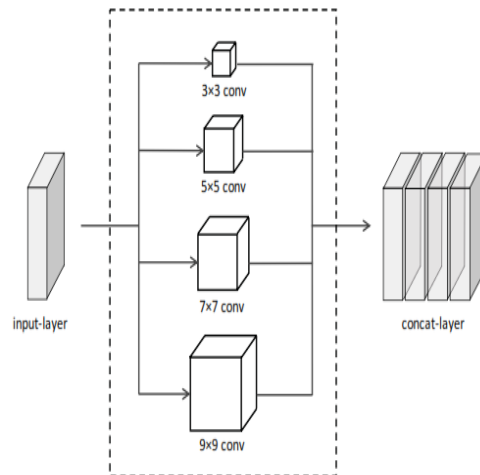


Figure 6. Multi-scale block with various size of kernel

Table 1. Lightweight U-Net architecture multi-scale convolutional network parameters.

Part 1	Type	Filters	Filter size	Output size
conv	Conv	64	9×9	(256,256,64)
	ReLU	-	-	
msb	MSB conv	4×16	(9/7/5/3)×(9/7/5/3)	(256,256,64)
	ReLU	-	-	
Max pool	Max pool	-	2×2	(128,128,64)
msb	MSB conv	4×32	(9/7/5/3)×(9/7/5/3)	(128,128,128)
	ReLU	-	-	
	MSB conv	4×32	(9/7/5/3)×(9/7/5/3)	
	ReLU	-	-	
Max pool	MAX pool	-	2×2	(64,64,128)
msb	MSB conv	4×64	(9/7/5/3)×(9/7/5/3)	(64,64,256)
	ReLU	-	-	
	MSB conv	4×64	(9/7/5/3)×(9/7/5/3)	
	ReLU	-	-	
Up-conv	Upsample	-	2×2	(128,128,128)
	Conv	128	2×2	
	ReLU	-	-	
conv	Conv	64	3×3	(128,128,128)
	ReLU	-	-	
	Conv	64	3×3	
	ReLU	-	-	
Up-conv	Upsample	-	2×2	(128,128,128)
	conv	64	2×2	
	ReLU	-	-	
conv	Conv	64	3×3	(128,128,128)
	ReLU	-	-	
	Conv	64	3×3	
	ReLU	-	-	
conv	Conv	2	3×3	(256,256,2)
	ReLU	-	-	
conv	Conv	1	1×1	(256,256,1)

BAA used a left-hand radiograph which is frequently demanded by kids assessment with different endocrinopathies or kids having malformation syndromes and as part of the planning procedures of orthopedic in which development of subsequent infant affects result. UNet2 suggested to tackle the need for more precise segmentation of the bone picture. The suggested architecture uses re-designed skip paths and profound oversight. Before any of this, for the previous segmentation, the k-means clustering is implemented. Semantic gap between encoder and decoder subnetwork feature maps is reduced by re-designing skip pathways which results in potentially simple optimization problem for optimizer to solve. Lightweight U-Net multi-scale convolutional architecture network is implemented to segment pediatric hand bone in X-ray picture and it has accomplished successful segmentation outcomes, particularly for the segmentation of tiny hand bones. In this work, pediatric bone imaging datasets is used to properly assess UNet1, UNet2, UNet3 and UNet+++. Even more chapter explains the simulations and the outcomes.

3 Experimental Results And Discussion

In the experimental part, the aim is to prove empirically that the proposed method are able to achieve similar performance levels with the original UNet while drastically increasing the speed of a forward pass than the existing methods.

4.1. metrics Used For Evaluation

Using specificity, sensitivity, Intersection over Union (IoU), dice coefficient are used to evaluate the results of segmentation.

IoU: It is expressed as,

$$IoU = \frac{(S_1 \cap S_2)}{(S_1 \cup S_2)}$$

In above equation, S_1 is results of segmentation result and S_2 is ground truth.

Sensitivity: Number of FN and TP are used to compute sensitivity as

$$sensitivity = \frac{TP}{TP + FN}$$

Specificity: specificity is defined as

$$sensitivity = \frac{TN}{TN + FP}$$

Where, true positive is represented as TP, false positive is represented as FP, true negative is represented as TN and false negative is represented as FN. Detection accuracy (DACC) is computed to evaluate the small bones detailed segmentation. It is expressed as,

$$DACC = \frac{N_s}{N_g}$$

Where, number of small bones of hand is represented as N_s which is segmented by network and number of small bones of hand in groundtruth is represented as N_g . Adjacent bones are not connected with segmented bones. In three ROIs, hand's small bones are located namely, Ulnar & Radius, Carpal and Phalangeal as shown in figure 7

Phalangeal ROIs includes Proximal phalangeal (Pro), Middle phalangeal (Mid) and Distal phalangeal epiphysis (Dis).

Carpal ROIs includes Scaphoid (Sca), Trapezium (Tra2), Trapezoid (Tra1), Lunate (Lun), Triquetral (Tri), Capitate (Cap), Hamate (Ham).

Ulnar & Radius ROIs includes Distal radius (Rad) Distal ulnar epiphysis (Uln).

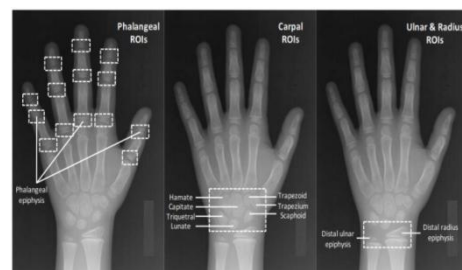


Figure 7. Hand image radiograph with superimposed regions of interest

In epiphyses of tubular and carpal bones, ossification centre analysis forms base for examination. Radius, ulna, proximal phalanges, middle phalanges and distal phalanges are included in this as shown in figure 7. Appearance of ossification centres or epiphyses can be delayed or accelerated by illness. Pediatric syndromes and endocrine disorders are managed by using BAA.

4.2. Experimental Results

DATASET: Digital Hand Atlas Database System is used for collecting dataset for evaluating accuracy of segmentation of proposed method. It is comprehensive X-ray and public dataset and it is used in automated skeletal bone age benchmarking. There are 1391 X-ray images of left-hands of children. Age group of children is less than 18 years. Based on race and gender, dataset is divided. Two expert radiologists gives two bone age values for every X-ray. In experimentation, excluded the images obtained from children with more than 7 years of age are, in order to compute the performance of segmentation. Exclusion of images are done due to the fact that, after 8 years, children's

hand small bones are started to merge. So, there will be only 429 images of children hand with less than 7 years age. Training dataset with 252 images, testing dataset with 88 images and validation dataset with 89 images are formed by dividing the dataset randomly without overlapping.

4.2.1. Comparison Of Performance of Segmentation on Different U-Net Based Network Architectures

With various architectures of U-Net, segmentation of hand bone results are compared with various number of operations in up and down sampling and u-Net++. Figure 8 demonstrates the pre-processing results and Figure 9 shows the k-means cluster based segmentation of bone image. Finally the Figure 10 shows typical segmentation results with the proposed CNN based U-Net. When compared with other networks, clustering done by proposed U-Net based on CNN, has produced better results. Small variations in input are not properly noticed by U-Net. So small bones cannot be segmented using U-Net effectively. Highly effective results are produced by proposed method.



Figure 8. Input bone image with pre-processing step



Figure 9. K-means based hand bone segmentation results

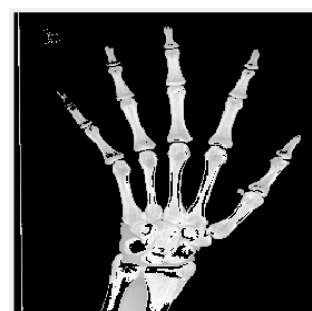


Figure 10. Results of Hand bone segmentation of various CNN with U-Net based network architecture.

With respect to specificity, sensitivity, IoU, dice similar performance in segmentation is shown by other methods except U-Net1 as demonstrated by figure 4.3. When compared with other networks, with less parameters, same performance of

segmentation is exhibited by U-Net with high computational efficiency. Proposed CNN based U-Net is evaluated in terms of segmentation accuracy using hand's small bones DACC, which is shown in figure 4.3.

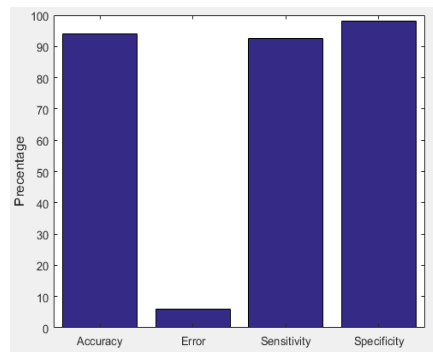


Figure 11. Results of small bones of hand of CNN with U-Net based network architecture

As denoted in Figure 11, the proposed method achieves a higher accuracy, sensitivity, specificity and low error rate on bone images. The results of CNN with U-Net is accuracy is 95%, sensitivity is 92%, specificity is 98% and error is 8%.

Multi-Scale Blob (MSBs) with different single size kernel are replaced by CNN with U-Net in order to enhance performance of segmentation. Experimentation results showed that, better performance is shown by CNN with U-Net when compared to single size kernel. With respect to specificity, sensitivity, IoU, dice, similar performance of segmentation is produced by MSB or CNN with single size kernel. In hand bone segmentation, better results are produced by proposed method as indicated by results, especially in hand's small bones.

4 Conclusion with future work

In X-ray images, for segmentation of pediatric hand bone, this worked proposed a U-Net architecture with k-means multi-scale convolutional network. It is a light weighted algorithm. Hand's small bones can be segmented with high accuracy. For assessing BAA, radiographic methods are used. Cause of imprecision is minimized by proposed method by considering X-ray image's quality. Proposer positioning of hand is more important. Small born bones appearances can be changed by wrong positioning of hand.

These methods are applied with scoring methods. Years and month representation of BAA is avoided and percentiles are used. It also considers the maturation difference between various population.

Proposed model's number of parameters are maintained by modified U-Net instead of U-Net. Best hyper parameter set can be computed in future. Medical images of various modalities can be used to evaluate the performance in future.

References

1. Gaskin CM, Kahn SL, Bertozzi JC, Bunch PM. Skeletal Development of the Hand and Wrist: A Radiographic Atlas and Digital Bone Age Companion: A Radiographic Atlas and Digital Bone Age Companion. Oxford University Press; 2011.
2. Zafar AM, Nadeem N, Husen Y, Ahmad MN. An appraisal of Greulich-Pyle Atlas for skeletal age assessment in Pakistan. J Pak Med Assoc. 2010;60(7):552-555.
3. Khan K, Elayappen AS. Bone Growth Estimation Using Radiology (Greulich-Pyle and Tanner-Whitehouse Methods) In: Preedy VR, editor. Handbook of Growth and Growth Monitoring in Health and Disease [Internet] New York: Springer; 2012. [cited 2013 Jul 13]. pp. 2937-53.
4. Kaplowitz P, Srinivasan S, He J, McCarter R, Hayeri MR, Sze R. Comparison of bone age readings by pediatric endocrinologists and pediatric radiologists using two bone age atlases. *PediatrRadiol*. 2010;41(6):690-693.
5. Szegedy, Christian, Wei Liu, YangqingJia, Pierre Sermanet, Scott Reed, DragomirAnguelov, DumitruErhan, Vincent Vanhoucke, and Andrew Rabinovich. "Going deeper with convolutions." In Proceedings of the IEEE conference on computer vision and pattern recognition, pp. 1-9. 2015.
6. R.V. Patil, K.C. Jondhale, "Edge based technique to estimate number of clusters in k-means color image segmentation," 3rd IEEE International Conference on Computer Science and Information

- Technology (ICCSIT), Vol. 2, pp. 117-121, 9 July 2010.
7. M. Mignotte, "Segmentation by Fusion of Histogram-Based K-Means Clusters in Different Color Spaces," in Proc. IEEE Trans. Image Processing, Conf., Vol. 17, pp. 780-787, May 2008.
 8. A. A. Z. Irani, B. Belaton, "A K-means Based Generic Segmentation System," 6th International Conference on Computer Graphics, Imaging and Visualization, Vol. 9, pp. 300-307, 11 August 2009.
 9. X. Wenzhu, X. Lihong, "A novel shot detection algorithm based on clustering," 2nd International Conference on Education Technology and 73 Computer (ICETC), Vol. 1, pp. 570-572, 22 June 2010.
 10. Z. Zhou, M. M. R. Siddiquee, N. Tajbakhsh, and J. Liang, "Unet++: A nested u-net architecture for medical image segmentation," in Deep Learning in Medical Image Analysis and Multimodal Learning for Clinical Decision Support: Springer, 2018, pp. 3-11.
 11. Zeng, Lingke, XiangminXu, BolunCai, SuoQiu, and Tong Zhang. "Multi-scale convolutional neural networks for crowd counting." In 2017 IEEE International Conference on Image Processing (ICIP), pp. 465-469. IEEE, 2017.
 12. Nair, V. and Hinton, G.E., 2010. Rectified linear units improve restricted boltzmann machines. In Proceedings of the 27th international conference on machine learning (ICML-10) (pp. 807-814).